Estuarine, Coastal and Shelf Science 281 (2023) 108209

Contents lists available at ScienceDirect

Estuarine, Coastal and Shelf Science

journal homepage: www.elsevier.com/locate/ecss

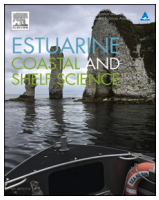

Connectivity patterns and gene flow among *Chelon ramada* populations

Esmeralda Pereira [a,*], Catarina S. Mateus [a], Maria J. Alves [b], Rita Almeida [a], Joana Pereira [a], Bernardo R. Quintella [c], Pedro R. Almeida [a,d]

[a] MARE – Centro de Ciências do Mar e do Ambiente / ARNET - Rede de Investigação Aquática, Instituto de Investigação e Formação Avançada, Universidade de Évora, 7002-554, Évora, Portugal
[b] Centro de Ecologia, Evolução e Alterações Ambientais (cE3c), Faculdade de Ciências & Museu Nacional de História Natural e da Ciência, Universidade de Lisboa, Lisboa, Portugal
[c] MARE – Centro de Ciências do Mar e do Ambiente, Faculdade de Ciências da Universidade de Lisboa / ARNET - Rede de Investigação Aquática /Departamento de Biologia Animal, Faculdade de Ciências, Universidade de Lisboa, Lisboa, Portugal
[d] Departamento de Biologia, Escola de Ciências e Tecnologia, Universidade de Évora, Évora, Portugal

ARTICLE INFO

Keywords:
Thinlip grey mullet
Catadromy
Population structure
Genetic diversity
Microsatellite markers

ABSTRACT

Catadromous species, such as the thinlip grey mullet *Chelon ramada* (Risso 1827), exhibit complex life history traits and migratory behaviours that have different repercussions at the population level and species genetic structure. To study the genetic variation and infer patterns of gene flow and population connectivity along species' distribution across the Northeast Atlantic coast and the Mediterranean Sea, 457 individuals from sixteen locations were genotyped using eleven microsatellite markers. The existence of a metapopulation with high gene flow was supported by the absence of significant genetic differentiation among locations or geographic clustering of samples. The Portuguese populations are important for the maintenance of connectivity among populations of the Mediterranean and Northeast Atlantic regions, as evidenced by the high degree of gene flow observed between the Portuguese coast and all populations from these two regions.

Our findings suggest that the thinlip grey mullet display a high dispersal capability, that combined with continuous habitat availability and large population numbers (low commercial exploitation in the Atlantic region), allow the maintenance of a unique genetic group.

1. Introduction

The thinlip grey mullet *Chelon ramada* (Risso, 1827) is a pelagic catadromous mugilid fish, widely distributed along the Northeast Atlantic coast, from the Norwegian coastline, down to Mauritania, on the African coast, including the Mediterranean and Black Sea, and the offshore islands of the Canaries, Azores, and Madeira (20–60° N, 18° E – 42° W) (Nelson, 2006). Despite *C. ramada's* preference to inhabit the upper estuaries (Thomson, 1966; Almeida, 1996), this species occurs in large numbers throughout coastal areas, and in brackish and freshwater environments (Thomson, 1966; McDowall, 1997). Moreover, *C. ramada* displays a great variability of habitat use patterns and migratory behaviours along the geographical range (Daverat et al., 2011; Pereira et al., 2021). The species' euryhalinity (Wallace, 1975; Almeida, 1996; Cardona et al., 2008), and high ecological plasticity (Bruslé, 1981; Almeida, 2003; Cardona, 2016), as well as the high abundance of available food resources contribute for its success. In the Mediterranean region, the maintenance of optimal or suitable environmental conditions throughout the annual cycle (e.g., higher habitat productivity and temperatures) and longer growing seasons, seem to induce a prolonged estuarine residence (Gross et al., 1988; Chauvet et al., 1992; Chapman et al., 2015). In contrast, in the Atlantic region, signs of a highly variable population dynamics were identified among the few studies using capture–recapture data (Oliveira and Ferreira, 1997; Ordeix et al., 2011; Lemonnier, 2019), biotelemetry (Almeida, 1996), and otolith microchemistry (Daverat et al., 2011). For instance, during the trophic migration, this species is frequently reported in freshwater habitats (Almeida et al., 1992; Sauriau et al., 1994; Oliveira and Ferreira, 1997) and recent Passive integrated transponder (PIT) technology and acoustic telemetry data from central Portugal showed that a fraction of the population returned annually to the same river stretch (unpublish data E. Pereira). The existence of what seems to be a certain degree of fidelity to the same river basin (unpublish data E. Pereira) unveils an even more complex migratory dynamic. Moreover, in terms of its reproductive

* Corresponding author.
E-mail address: ecdp@uevora.pt (E. Pereira).

https://doi.org/10.1016/j.ecss.2022.108209
Received 11 August 2022; Received in revised form 25 December 2022; Accepted 30 December 2022
Available online 2 January 2023

biology, different spawning periods have been reported throughout its distribution. The presence of *C.ramada'* fry in the estuary is reported from December to July (reviewed in Koutrakis, 2016), a time frame that is attributed to the extended period of spawning (between September and January) and the existence of a protracted recruitment that ranges from four to six weeks (Claridge et al., 1986, Bartulović et al., 2007).

Catadromous iteroparous life cycle characteristics, such as the spawning location, the mixed spawning cohorts, the protracted spawning migration, high larval dispersal (Jerry and Baverstock, 1998), together with the unpredictability of oceanic conditions, are known to promote low levels of population structure or panmixia over large geographical scales (e.g., anguillid eels, Als et al., 2011). However, species specific traits, such as different habitat use patterns/migratory profiles (Waples, 1998, Frisk et al., 2014; Hughes et al., 2014), dispersal capabilities of different life-stages (Leclerc et al., 2008; Islam et al., 2018) and recruitment' success (Werner and Gilliam, 1984; Whitfield et al., 2012; Feutry et al., 2013; Gallagher et al., 2018) can promote restricted gene flow and isolation by distance. Ultimately, it is the sum of these factors that will shape at different degrees, the demographic connectivity among populations, and the species population structure (O'Dwyer et al., 2021; Baselga et al., 2022).

Highly polymorphic microsatellite markers have been widely applied to study fine scale population structure of fishes (e.g. Shen et al., 2011; Cuéllar-Pinzon et al., 2016), genetic differentiation at different geographical scales (e.g. Colín et al., 2020) and demographic dynamics (e.g., Duong et al., 2019; Guo et al., 2022). In this sense, this molecular tool provides an opportunity to assess how complex life history traits and migratory dynamics shape the population structure and connectivity (Kasapidis et al., 2012; Limborg et al., 2012). Previous studies using microsatellites on distinct mugilid species, such as *Mugil cephalus* L., *Mugil liza* (Valenciennes, 1836) and *Mugil curema* (Valenciennes, 1836), have reported different degrees of genetic differentiation along species' distribution. While some authors observed a total absence of genetic structure and existence of a unique genetic stock (e.g., Huey et al., 2013; Cossu et al. 2021), others have described scenarios of population fragmentation (e.g., Jamandre et al., 2009; Lui et al., 2009) and chaotic spatial distribution (e.g., Brito, 2018). In the particular case of *C.ramada*, the implications of a variable and complex population dynamic, particularly associated with different migratory profiles in the Atlantic region and the asynchronous spawning and juvenile recruitment, as well as the influence of local historical events on species' genetic structure remains unknown. Therefore, with the aim to investigate *C.ramada* genetic structure and infer the connectivity patterns among populations, the present study uses microsatellite DNA markers to analyze the genetic diversity, the genetic differentiation, and gene flow among populations, and test the hypothesis that the species maintains a unique genetic group along its distribution range. A more detailed spatial analysis in terms of sampling locations was directed towards the Iberian coast, more precisely to Portugal, as it may act as a transition zone between the Atlantic-Mediterranean populations and a diversity of migratory profiles seem to occur in this region (unpublish data E. Pereira).

To our knowledge, the present study represents the first assessment of population genetic structure and dispersal dynamics of *C.ramada* along its distribution range. Acknowledging the current human pressure on coastal and continental aquatic systems and under a climate change scenario, this information is essential to predict genetic population trends, demographic dynamics, and support fisheries management.

2. Material and methods

2.1. Sampling

Between 2020 and 2021, a total of 457 samples of *C. ramada* were collected from sixteen sampling sites: one in the Celtic Sea (Ireland), one in the North Sea (Belgium), one in the Bay of Biscay (France), nine along the Portuguese coast, two in the Western Mediterranean (Italy) and two in the Eastern Mediterranean (Greece) regions (Fig. 1; Table 1). Fin clip samples were immediately collected and individually stored in a tube with absolute ethanol and remained at −20 °C until DNA extraction.

The two sampling sites from Italy and from Greece were pooled as representatives of the geographical areas of Western Mediterranean and the Eastern Mediterranean, respectively.

2.2. Amplification and genotyping of microsatellite loci

Total genomic DNA was extracted using DNeasy® Blood and Tissue kit (Qiagen) following the manufacturer's instructions. DNA quality and quantity were evaluated using a Thermo Scientific NanoDrop™ 1000 Spectrophotometer. Eleven nuclear microsatellite loci originally designed for the species *Mugil cephalus, Planiliza haematocheilus* (Temminck and Schlegel, 1845) and *Chelon affinis* (Günther, 1861) were selected from Xu et al. (2009, 2010), Shen et al. (2010) and Liu et al. (2016) (Supplementary Table S1). The optimization for genotyping was performed from the general protocol described in Pacheco-Almanzar et al. (2017) and Liu et al. (2019). The primer sets were grouped into three multiplex reactions and the reverse primers were labelled with fluorescent dye (6-FAM, HEX, ATTO550 or ATTO565) at the 5′ end. The polymerase chain reactions (PCR) were set up in final volumes of 12 μl containing 1 μl of genomic DNA (40 ng/μl), 0.6 units of My TaqTM DNA polymerase (Bioline), 1.2 μl of 5 x My Taq Reaction Buffer (Bioline), 0.4 μM for each primer and ultrapure water. The PCR reactions were run for 29–35 cycles (Supplementary Table S1) on a Gene Explorer thermal cycler (model GE-96G) and with the exception of La195, it included an initial activation step at 95 °C for 5 min, denaturation at 94 °C for 30 s, primer annealing at 54 °C for 45s, extension at 72 °C for 45 s and final extension at 72 °C for 10 min. Protocol for La195 comprised an initial activation step at 95 °C for 2 min, denaturation at 94 °C for 30 s, primer annealing at 54 °C for 45s, extension at 72 °C for 60 s and final extension at 72 °C for 10 min.

Samples were genotyped in an ABI 3730 XL Genetic Analyzer and fragments were sized with GeneScan™-500 LIZ™ Size Standard. The assignment of alleles was performed using the GeneMapper v. 3.7 software (Applied Biosystems).

2.3. Data analyses

Genotypes were inspected for the presence of null alleles, stuttering and large allele drop-out using MICRO-CHECKER v.2.2.3 (van Oosterhout et al., 2004) and subsequently visually examined for correction. Departure from Hardy–Weinberg equilibrium (HWE) and linkage disequilibrium were inspected using ARLEQUIN v.3.5.2.2 (Excoffier and Lischer, 2010; 10^4 permutations). The probability values of each test were corrected with the sequential Bonferroni correction. The pairwise F_{ST} values from the original data and the data with null alleles correction (corrected F_{ST}-ENA, ENA method) were obtained using FREENA (Chapuis and Estoup, 2007) (10^4 permutations) and compared to verify the influence of null alleles (Chi-square test).

2.3.1. Genetic diversity

The mean number of alleles per locus (MNa), the mean number of private alleles (Np), the mean observed (Ho), expected (He) and unbiased expect heterozygosities (uHe) were calculated with GenAlEx v.6.5 (Peakall and Smouse, 2012). The mean allelic richness (Ar) and the inbreeding coefficient (F_{IS}), with 95% confidence intervals (10^4 bootstrap replicates) were estimated with the diveRsity package in R v.4.1 (Keenan et al., 2013). Differences among populations were evaluated based on pairwise F_{ST} values computed (10^4 permutations) in ARLEQUIN v.3.5.2.2. Pairwise F_{ST} values were compared with Jost's D and GST values estimated (10^4 permutations) in GenAlEx v.6.5.

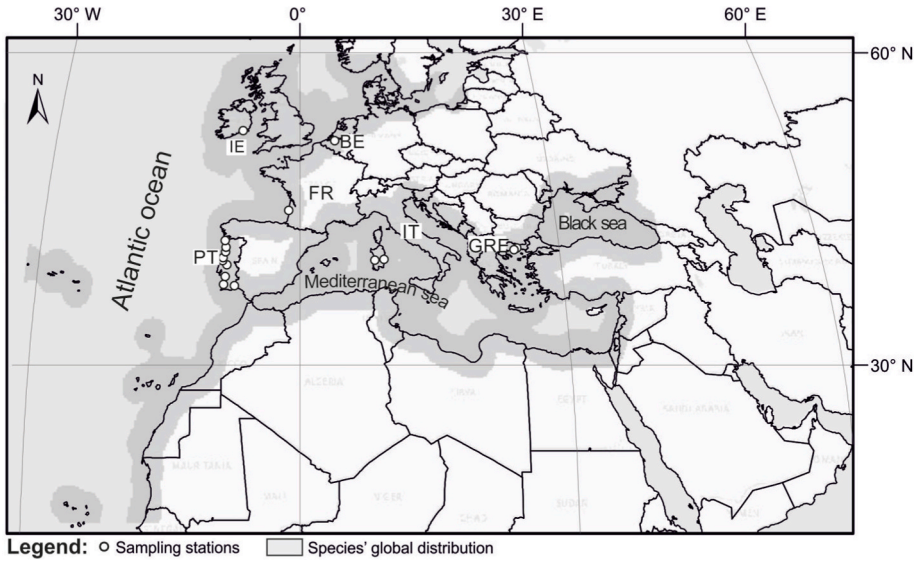

Fig. 1. Geographic location of the sampling sites where *Chelon ramada* samples were obtained. The respective countries, namely Ireland (IE), Belgium (BE), France (FR), Portugal (PT), Italy (IT) and Greece (GR) are identified.

Table 1
Origin and number of *Chelon ramada* samples collected per location. When appropriate, sample provider is identified.

Country	Location	ID	Coordinates		N. of samples	Sampling year	Sample provider
			X	Y			
[Celtic Sea]							
Ireland	Waterford Harbour	IE	6°59′15.7″W	52°09′07.1″N	26	2020	William Roche
[North Sea]							
Belgium	Scheldt basin	BE			29	2020	Jan Breine
	[Doel]		4°16′08.9″E	51°18′36.5″N			
	[Steendorp]		4°16′26.3″E	51°07′25.7″N			
	[Zuienkerke]		3°04′55.2″E	51°18′22.3″N			
[Bay of Biscay]							
France	Arcachon Bay	FR	1°11′40.7″W	44°40′36.4″N	20	2020	Authors
[Portuguese coast]							
Portugal	Lima basin	PT_LM	8°40′51.9″W	41°43′29.8″N	36	2020	Commercial fisherman
	Douro basin	PT_DO	8°31′52.1″W	41°06′13.9″N	35	2020	Commercial fisherman
	Vouga basin	PT_VO	8°33′36.4″W	40°40′22.0″N	35	2020	Commercial fisherman
	Mondego basin	PT_MO	8°51′23.7″W	40°08′32.4″N	35	2020	Authors
	Lis basin	PT_LD	8°51′45.9″W	39°51′50.3″N	35	2020	"Pró-Lis friends"/Authors
	Tejo basin	PT_TJ	8°12′30.2″W	39°27′00.2″N	35	2020	Commercial fisherman
	Sado basin	PT_SD	8°31′10.8″W	38°22′19.2″N	34	2020	Authors
	Mira basin	PT_MR	8°40′15.6″W	37°37′23.9″N	35	2020	Authors
	Guadiana basin	PT_GD	7°27′58.9″W	37°28′18.4″N	28	2020	Commercial fisherman
[Western Mediterranean]							
Italy	Santa Giusta	IT	8°35′32.3″E	39°51′58.7″N	30	2021	Laura Mura
	Tortoli		9°40′18.1″E	39°56′40.9″N	9		
[Eastern Mediterranean]							
Greece	Lake vistonida	GR	25°06′40.3″E	41°02′37.8″N	22	2021	Emmanuil Koutrakis
	Lagoon keramoti		24°42′37.9″E	40°52′00.9″N	13		

2.3.2. Genetic structure

The distribution of the genetic variation among and within populations was analysed through a locus-by-locus Analysis of Molecular Variance (AMOVA; 20^4 permutations, p-value <0.05) using allelic frequencies as genetic distance, in ARLEQUIN v.3.5.2.2. Patterns of differentiation between locations were visualised with a principal coordinates analysis (PcoA) performed in GenAlEx v.6.5 and a three-dimensional factorial correspondence analysis (3D-FCA) was performed in GENETIX 4.05 (Belkhir et al., 2004). Population genetic structure was assessed through a Bayesian-model-based cluster analysis using STRUCTURE v.2.3.4 (Pritchard et al., 2000). Simulations were run using the admixture model of population structure, with correlated allele frequencies (LOCPRIOR model). The number of clusters (K) was set between 1 and 14 and for each K, 10 independent simulations were performed with an initial burn-in period of 10^5, followed by 10^6 Markov Chain Monte Carlo (MCMC) algorithm iterations. The most likely number of genetic discrete populations (K) was determined using the likelihood distribution (Pritchard et al., 2000) and the ΔK method (Evanno et al., 2005), using STRUCTURE HARVESTER (Earl and Vonholdt, 2012). The results were visualised in DISTRUCT v1.1 (Rosenberg, 2004).

2.3.3. Migration analysis

Isolation-by-distance (IBD) was analysed through Mantel's test (9999 permutations) in GenAlEx v.6.5. Shortest route distances (km) between sampled populations were estimated in Google Earth and plotted against genetic distance (pairwise F_{ST}'s). Recent genetic bottlenecks were evaluated with the Wilcoxon sign-rank test for

heterozygosity excess applied under two different models, namely, the two-phase model (TPM; proportion of SMM 70% and variance 30%) and the stepwise mutation model (SMM) (5000 simulations), using the program Bottleneck 1.2.02 (Piry et al., 1999). The relative gene flow along species distribution and directional components of genetic divergence between pairs of populations were analysed with divMigrate function of diversity package in R v.4.1, based on F_{ST} measure between different countries.

3. Results

3.1. Genetic diversity levels

A total of 121 alleles with an average of 11 alleles per locus were observed with the eleven loci. The number of alleles per locus ranged from three (Muce16 and Muce26) to 24 (Muce 80) (Supplementary Table S2). Sixteen out of 154 locus-by-population tests exhibited significant departure from HWE, but none of them remained significant after correction for multiple tests (Supplementary Table S2). The microsatellite loci Mce6 and La195 showed signs of stuttering and null alleles for the populations from the Douro Basin, Portugal (PT_DO) and Ireland (IE), respectively. The Mce6 locus displayed signs of null alleles in the Portuguese basin: Mondego (PT_MO), Lima (PT_LS) and Sado (PT_SD) and La195 in PT_MO. Signs of null alleles were also identified in Muce 80 for PT_DO and Muce55 for Vouga Basin, Portugal (PT_VO). However, the genetic structure was not affected by including these loci in the analysis (Supplementary Table S3).

Genetic diversity levels were similar across the populations studied (Table 2). The mean number of alleles per location ranged between 7.000 (France-FR/Ireland-IE) and 8.273 (Mira Basin, Portugal-PT_MR). In total, 18 private alleles were identified, and FR population displayed the highest value (3) of private alleles. The average allelic richness value was the highest in PT_MR (6.490) and the lowest in PT_DO (5.820). The observed and expected heterozygosity per population varied from 0.547 (PT_DO) to 0.655 (Belgium-BE), and from 0.595 (PT_DO) to 0.638 (Guadiana Basin, Portugal- PT_GD), respectively. All populations showed an inbreeding coefficient (F_{IS}) close to zero, which is associated with low levels of inbreeding (homozygotes' excess).

F_{ST} values were low and ranged between −0.005 (PT_SD↔ FR) and 0.010 (PT_LM↔ IE) (Table 3). After Bonferroni correction, no genetic differences were found among populations. Similarly, the GST ranged from −0.004 (FR ↔ PT_MR) to 0.006 (IE↔ Tagus Basin, Portugal-PT-TJ) and Jost's D values between −0.015 (FR ↔ PT_MR) to 0.019 (IE↔PT_TJ) (Supplementary Tables S4 and S5).

3.2. Population genetic structure

Almost all the genetic variation was explained within populations (AMOVA, 99.7%, p-value<0.001; Table 4). No clear groups were identified through the principal coordinates analysis (PCoA), whose first and second axis explained respectively 14.3% and 15.6% of the variation (Fig. 2). A large overlap among all samples and the lack of an obvious cluster were also identified using three-dimensional factorial correspondence analysis (4.15% of the overall variation explained).

The Bayesian cluster analysis has indicated two clusters (Fig. 3) based on ln P(D) and AK scores across population and showed that nearly each individual was assigned roughly in equal proportions to each of the clusters (Fig. 3, Table 5), excluding any geographical or genetic structure.

3.3. Migration analysis

According to the Mantel test, no significant correlation (R = 0.23, P > 0.05) was observed between genetic distance determined as $F_{ST}/(1-F_{ST})$ and geographical distance based on all loci. There was no evidence of recent population bottleneck under the TPM and SMM evolutionary models and the distributions of allele frequencies were L-shaped ('mode-shift' indicator), which suggest that *C.ramada'* populations were stable and in mutation-drift equilibrium (Table 6).

In terms of the relative migration network analysis, the strongest level of gene flow was identified between the Western Mediterranean and the Portuguese coast, with the highest rates of migrants being recorded towards the Atlantic. Yet different levels of connectivity and symmetry were found when considering the Italian and the Greek populations. Italy showed the highest levels of relative migration to and from Portugal, with mean relative migration of 1.0 and 0.7, respectively, while Greece maintained a symmetrical mean migration of approximately 0.6. A similar magnitude of relative migration was also observed in the Northeast Atlantic, either between Belgium and Portugal, and from France to Portugal. Within both Western Mediterranean and the remaining Northeast Atlantic populations, a relative migration of at least, 0.20 to 0.30, with in most cases, symmetric levels of gene flow (m) were maintained. The lowest values of gene flow were reported for Ireland (Fig. 4, Table 7).

4. Discussion

The present work provides relevant information on the diversity, structure, and genetic variability of *C. ramada* populations inhabiting the Northeast Atlantic coasts and the Mediterranean Sea. In terms of the allelic richness (Ar = 5.820–6.490) and the genetic diversity observed (Ho = 0.540–0.655), the values obtained were relatively low and homogeneous throughout the distribution range. Low values have been reported for other mugilid species, such as *Chelon auratus* Risso, 1810 (Ar = 6.167–6.33; Ho = 0.369–0.53; Behrouz et al., 2018) and *Chelon saliens* Risso, 1810 (Ar = 5.7–8; Ho = 0.68–0.83; Naderi et al., 2017), using non-species-specific markers at a small spatial scope. While higher values were reported for *L. affinis* along the eastern and southern China

Table 2
Genetic diversity of *Chelon ramada* estimated using 11 microsatellite loci: mean number of alleles (Mna); mean allelic richness (Ar), mean number of private alleles (Np), observed heterozygosity (Ho), expected heterozygosity (He), mean unbiased estimate of expected heterozygosity (uHe) and Inbreeding coefficient (F_{is}), with lower and upper 95% confidence intervals (F_{is}_Low and F_{is}_High) determined with 1000 bootstrap replicates). HWE = probability of deviation from Hardy-Weinberg equilibrium with Bonferroni correction (p = 0.00034). Codes of geographic locations in Table 1.

	IE	BE	FR	PT_LM	PT_DO	PT_VO	PT_MO	PT_LS	PT_TJ	PT_SD	PT_MR	PT_GD	IT	GR
Mna	7.000	7.182	7.000	7.091	7.182	7.364	7.091	7.636	7.545	7.273	8.273	7.636	7.182	7.727
Ar	6.030	6.200	6.000	5.940	5.820	6.000	6010	6.110	6.110	6.030	6.490	6.330	5.890	6.340
MNp	0.000	0.000	0.273	0.091	0.182	0.091	0.091	0.091	0.091	0.091	0.182	0.091	0.182	0.182
(Np)	(0)	(0)	(3)	(1)	(2)	(1)	(1)	(1)	(1)	(1)	(2)	(1)	(2)	(2)
Ho	0.598	0.655	0.626	0.636	0.547	0.608	0.597	0.616	0.62	0.621	0.613	0.653	0.617	0.631
He	0.620	0.631	0.638	0.622	0.595	0.627	0.631	0.601	0.612	0.624	0.629	0.638	0.605	0.632
uHe	0.632	0.642	0.655	0.631	0.604	0.636	0.640	0.610	0.621	0.633	0.638	0.649	0.613	0.642
HWE	0.035	0.431	0.003	0.302	0.667	0.773	0.014	0.019	0.828	0.746	0.082	0.017	0.937	0.577
F_{IS}	0.0346	−0.0382	0.0194	−0.0225	0.0813	0.0309	0.0528	−0.0234	−0.0124	0.0055	0.0255	−0.0239	−0.0186	0.0019
F_{is}_Low	−0.021	−0.087	−0.043	−0.073	0.029	−0.025	−0.017	−0.096	−0.082	−0.060	−0.027	−0.080	−0.078	−0.054
F_{is}_High	0.086	0.009	0.079	0.029	0.134	0.089	0.124	0.048	0.058	0.073	0.076	0.025	0.043	0.055

Table 3
Pairwise estimates of F_{ST} values among *Chelon ramada* populations (below diagonal) and corresponding P-values (above diagonal; $p < 0.00034$ after Bonferroni correction). Codes of geographic locations in Table 1.

	IE	BE	FR	PT_LM	PT_DO	PT_VO	PT_MO	PT_LS	PT_TJ	PT_SD	PT_MR	PT_GD	IT	GR
IE	-	0.504	0.405	0.021	0.089	0.068	0.024	0.051	0.010	0.260	0.255	0.135	0.052	0.087
BE	0.000	-	0.350	0.292	0.036	0.755	0.065	0.051	0.291	0.567	0.219	0.264	0.101	0.035
FR	0.002	0.001	-	0.762	0.367	0.805	0.893	0.269	0.549	0.876	0.993	0.454	0.425	0.279
PT_LM	0.010	0.001	−0.003	-	0.016	0.431	0.162	0.099	0.684	0.678	0.248	0.232	0.697	0.013
PT_DO	0.008	0.009	0.003	0.010	-	0.361	0.099	0.038	0.171	0.469	0.678	0.087	0.087	0.335
PT_VO	0.007	−0.003	−0.003	0.000	0.002	-	0.583	0.128	0.624	0.792	0.751	0.585	0.658	0.391
PT_MO	0.010	0.006	−0.004	0.003	0.006	0.000	-	0.052	0.422	0.854	0.553	0.509	0.206	0.103
PT_LS	0.008	0.006	0.003	0.004	0.008	0.004	0.006	-	0.025	0.069	0.090	0.515	0.331	0.010
PT_TJ	0.012	0.001	−0.001	−0.002	0.004	−0.001	0.001	0.007	-	0.657	0.253	0.048	0.528	0.050
PT_SD	0.003	-0.001	−0.005	−0.002	0.001	−0.002	−0.003	0.005	−0.002	-	0.943	0.570	0.296	0.496
PT_MR	0.003	0.003	−0.009	0.002	−0.001	−0.002	0.000	0.005	0.002	−0.004	-	0.291	0.105	0.273
PT_GD	0.005	0.002	0.000	0.002	0.006	−0.001	0.000	−0.001	0.007	−0.001	0.002	-	0.554	0.258
IT	0.007	0.004	0.000	−0.002	0.006	−0.001	0.003	0.001	−0.001	0.001	0.004	−0.001	-	0.047
GR	0.006	0.007	0.003	0.009	0.002	0.001	0.005	0.009	0.006	0.000	0.002	0.002	0.006	-

Table 4
AMOVA of *Chelon ramada* populations structure.

Source of variation	d.f.	Sum of squares	Variance Components	P-value	Percentage of variation
Among populations	13	52.03	0.01	0.020	0.25
Within populations	900	3090.15	3.43	0.000	99.75
Total	913	3142.18	3.44		

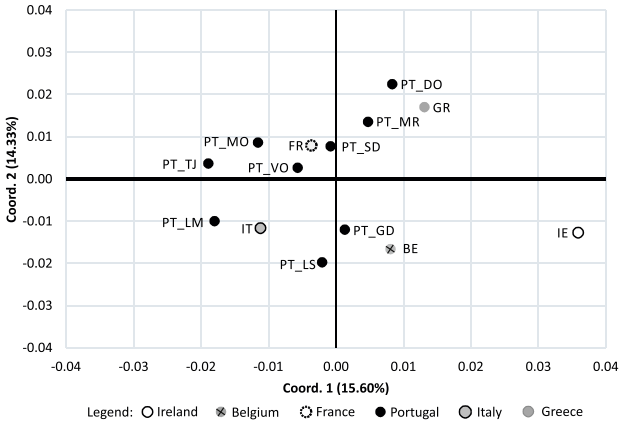

Fig. 2. Principal coordinates analysis plot (PCoA) based on the Pairwise estimates of F_{ST} values among *Chelon ramada* range populations. Codes of geographic locations in Table 1.

(Ar = 14.8–18.2; Ho = 0.59–0.805), using species-specific markers (Liu et al., 2019). For the cosmopolitan flathead mullet (*M. cephalus*), the most widespread species among the family Mugilidae, higher allelic richness (Xu et al., 2010; Shen et al., 2010, 2011; Liu et al., 2016) as well as higher genetic diversity were reported in restricted areas such as the Gulf of Mexico and Mexican Pacific (Ho = 0.692–0.840; Colín et al., 2020), New Zealand (Ho = 0.76–0.93; Brito, 2018) and Sardinia Island (Ho = 0.78–0.83; Cossu et al., 2021). Considering that the present work covers most of the *C. ramada* distribution (except the African coast), our results most probably reflect the low polymorphism of some microsatellite loci used, rather than small populations size or recent population declines.

Regarding *C. ramada's* genetic structure, the low differentiation among populations (AMOVA/pairwise F_{ST} results) and the lack of genetic partitioning (Bayesian clustering) provide evidence for a unique genetic group spread across the Northeast Atlantic coast and Mediterranean Sea. Among most mugilid species, microsatellite data has revealed distinct degrees of genetic differentiation depending on the geographic regions and study' spatial scope. For instance, in one of the most studied mugilid species, *M. cephalus*, the origin of three cryptic

Table 5
Proportion of membership of each predefined *Chelon ramada* population in each of the two inferred clusters from STRUCTURE analysis. Codes of geographic locations in Table 1.

Population	Inferred Clusters		Number of individuals
	1	2	
IE	0.288	0.712	26
BE	0.267	0.733	29
FR	0.277	0.723	20
PT_LM	0.217	0.783	36
PT_DO	0.215	0.785	35
PT_VO	0.221	0.779	35
PT_MO	0.255	0.745	35
PT_LS	0.233	0.767	35
PT_TJ	0.333	0.767	35
PT_SD	0.239	0.761	34
PT_MR	0.288	0.712	35
PT_GD	0.297	0.703	28
IT	0.205	0.795	39
GR	0.275	0.725	35

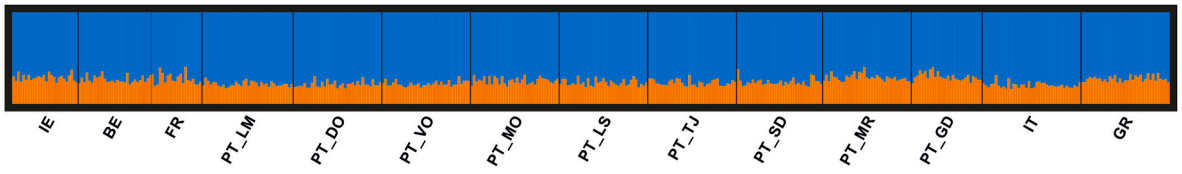

Fig. 3. Assignment test for *Chelon ramada* with eleven microsatellite data from the distribution range along the Northeast Atlantic and the Mediterranean region, computed under the admixture model with correlated allelic frequencies in STRUCTURE. Each individual is represented by a vertical bar and the proportion of each bar assigned to the colour orange and blue represents the probability that an individual is assigned to the inferred clusters (K = 2). Codes of geographic locations in Table 1. (For interpretation of the references to colour in this figure legend, the reader is referred to the Web version of this article.)

Table 6
Proportion of membership of each predefined *Chelon ramada* population in each of the two inferred clusters from STRUCTURE analysis. Codes of geographic locations in Table 1.

Population	Wilcoxon sign-rank test		Mode Shift distribution
	TPM	SMM	
IE	0.385	0.947	Normal L-shaped
BE	0.053	0.461	Normal L-shaped
FR	0.681	0.997	Normal L-shaped
PT-LM	0.074	0.840	Normal L-shaped
PT-DO	0.681	0.992	Normal L-shaped
PT-VO	0.232	0.989	Normal L-shaped
PT-MO	0.139	0.817	Normal L-shaped
PT-LS	0.615	0.988	Normal L-shaped
PT-TJ	0.577	0.998	Normal L-shaped
PT-SD	0.183	0.897	Normal L-shaped
PT-MR	0.348	0.991	Normal L-shaped
PT-GD	0.382	0.999	Normal L-shaped
IT	0.246	0.997	Normal L-shaped
GR	0.382	0.973	Normal L-shaped

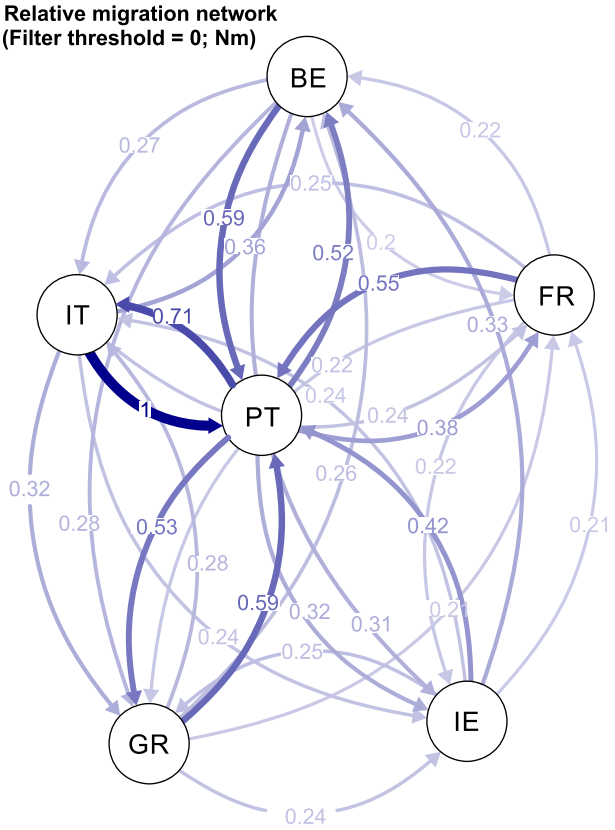

Fig. 4. Relative migration network among *Chelon ramada* populations. Arrows indicate direction of gene flow among populations and respective nm value (i.e., estimate of the gene flow from the population in the rows to the populations in the columns; ranges between 0 and 1. Codes of geographic locations in Table 1.

species in Pacific Northwest was attributed to complex interaction of contemporary processes and historical events, as sea level and temperature fluctuations during Plio-Pleistocene epochs (Shen et al.,2011), while in New Zealand coast, Brito (2018) identified a chaotic pattern that seems to be associated with seasonal variability in the mortality rates of juveniles, spawning behaviour and philopatry. On the other hand, in the Eastern Australian coast no genetic structuring was found,

Table 7
Estimates of Nm values (i.e., estimate of the gene flow from the population in the rows to the populations in the columns; ranges between 0 and 1) among *Chelon ramada* populations. Codes of geographic locations in Table 1. Values of Nm higher than 0.500 are displayed in bold.

From/To	IE	BE	FR	PT	IT	GR
IE	-	0.330	0.210	0.425	0.239	0.249
BE	0.310	-	0.201	**0.590**	0.272	0.286
FR	0.219	0.221	-	**0.555**	0.252	0.219
PT	0.322	**0.516**	0.379	-	**0.715**	**0.530**
IT	0.245	0.356	0.242	**1**	-	0.323
GR	0.240	0.261	0.214	**0.593**	0.279	-

following the pattern of other marine species present in the same region (panmixia) (Huey et al., 2013). Furthermore, in a smaller geographic coverage as the Sardinia Island (northwestern Mediterranean), Cossu et al. (2021) also identified the lack of genetic structuring and the existence of a unique genetic stock. Interestingly, Colín et al. (2020) observed panmictic populations in the Gulf of Mexico and two different clusters in the Mexican Pacific (Mexican Tropical Pacific/Chiapas–Nicaragua ecoregions) that may have been originated by ecological barriers such as the Tehuanos winds present during the spawning season (instead of philopatry). Thus, it can be argued that for *M. cephalus*, the genetic structure observed in the Atlantic (Gulf of Mexico) and Pacific coasts is the result of contemporary and historical oceanographic processes that may act as efficient barriers to larval dispersion and gene flow. For other grey mullets as *M. curema*, Ávila-Herrera et al. (2021) described the existence of four genetic groups in the Gulf of Mexico and Mexican Pacific, a pattern consistent with the oceanic conditions. Mai et al. (2014) identified distinct population clusters in *Mugil liza* along the South American Atlantic coast, that are eventually attributed to the existence of specifics oceanographic conditions and marine boundaries that may restrict gene flow.

In the present case, the maintenance of a unique genetic population throughout an extensive area (from Ireland to Greece) seem to reflect a combination of factors such as continuous habitat availability, large effective population sizes and life history traits that promote a strong dispersal ability and mixing gene pools, narrowing the impact of the genetic drift (Waples, 1998; DeWoody and Avise, 2000; Maes and Volckaert, 2007). A long longevity and an iteroparous strategy with a reproductive effort that is split between several events during a protracted spawning season (asynchronous spawning), a highly mixed spawning cohorts (Maes and Volckaert, 2007; Pacheco-Almanzar et al., 2017), as well as a planktonic larvae stage of 4–6 weeks (Oren, 1981; Yoshimatsu et al., 1993) and different stage' dispersal abilities, are expected to be the major forces driving the maintenance of the low genetic differentiation. Species' high dispersal ability is emphasised by the symmetrical gene flow observed in the relative migration network analysis, that support the existence of a flux of migrants against the main currents and suggest that species dispersion does not rely exclusive on passive larvae dispersion but also on the swimming capacity of recruits and the presence of migratory profiles among adults. During the early life stages in marine environment, a long-distance dispersal is expected to occur with the passive dispersal of pelagic larvae through the ocean currents (Jerry and Baverstock, 1998; Neethling et al., 2008; Kaimuddin et al., 2016) and later with the active (Harrison and Cooper, 1991) and assisted (by the flood tidal transport) dispersion of postflexion larvae to the nursery areas. During this period, olfactory clues are used to approach coastal areas including estuaries (Mires et al., 1974; Kingsford and Suthers, 1994), and reach these nursery areas as recruits. Jonsson and Jonsson (2008) reported the presence of *C. ramada* juveniles in a small brook in southern Norway and considering the closest spawning locations, the authors hypothesized that during their first year of growth at sea those animals may have dispersed from up to 900 km.

In terms of adult dispersion, the data available from the marine environment is scarce. However, otolith microchemistry analyses have

revealed a wide range of habitat shifts within *C. ramada* lifetime, an ability to move quickly between habitats and the existence of a population' fraction with preference for high salinity environments (Daverat et al., 2011). Telemetry data from adult *M. cephalus* migration in North Carolina also showed that two months before spawning, a small proportion of individuals was able to move to other estuaries located up to 860 km away from the tagging sites (Bacheler et al., 2005). Thus, despite the evidence of a certain degree of fidelity of *C. ramada* individuals to a specific watershed (unpublish data E. Pereira), the genetic homogenization at regional scales and an intermittent gene flow over large distances could also be promoted by sporadic migration and migratory displacements of adults along the coast. Moreover, considering the large distances travelled and the potential biogeographic barriers present in the studied area, species dispersal may also benefit from the relaxation of environmental conditions of ocean fronts during spawning migration, larva development and recruitment. In fact, between the Mediterranean Sea and the Atlantic Ocean, the Almeria-Oran front (AOF) has been identified as one of the major barriers to gene flow in species such as the *Trachurus picturatus* (Bowdich, 1825), the *Engraulis encrasicolus* L. or the *Xiphias gladius* L., but the migration analysis performed in the present study showed high levels of relative migration of *C.ramada* between both regions. Probably benefiting from the winter relaxation of the AOF (Tintoré and La Violette, 1988) that occurs during the peak of the planktonic larval phase and recruitment. However, the lower levels of relative migration observed between *C.ramada* population from the Eastern and Western Mediterranean (reported here), indicate that in central Mediterranean, species dispersion may be influenced by oceanographic features (Sá-Pinto et al., 2012 and references therein). Particular by the complex currents systems associated with the formation of the large mesoscale anticyclonic gyre eastwards towards Sicily Channel (Palero et al., 2008; Menna et al., 2019), whose effects can be enhanced by the prevalence of possible species' dispersal routes as described for *M. cephalus* (Durand et al., 2013). In the same way, the lower values of relative migration observed in the Northeast Atlantic coast may reflect the influence of the ocean currents, namely the northward residual current that flows through the English Channel into the Southern Bight of the North Sea (Prandle et al. 1996, Gysels et al., 2004) and the southern branch of the Gulf Stream that split towards Britain and continental Europe (Bower et al., 2002; Jakobsen et al., 2003; Palero et al., 2008). Nonetheless, even when gene flow seems to be hindered by ocean currents, *C. ramada* is able to maintain a minimum relative migration of at least 0.20 that seems to prevent genetic differentiation and subsidise genetic vigour into river systems.

Beyond the identification of a unique genetic population, one of the major findings of the present study was the consistently high level of gene flow between the Portuguese coast and all the populations studied. These results must be interpreted with caution as the spatial sampling was directed towards Portugal and the low resolution in the other regions may contribute to an incomplete view. Nonetheless, the relative gene flow along species distribution and directional components of genetic divergence showed that the Portuguese coast can play a pivot role in the maintenance of the low genetic structure reported. Since each of the Northeast Atlantic populations analysed (i.e., Ireland, Belgium, and France) displayed higher relative migration with the Portuguese coast rather than with each other, it can be hypothesized that preferential spawning areas may be located in this region. The upwelling zones with nutrient-rich waters that promote the primary production, and ensure high food availability, may attract adult thinlip grey mullets from different river basins. The opposite flux of migrants is expected to be mostly promoted by the Shelf Edge Current, flowing from north-western Africa to Norway, that provides a means for the dispersal of the planktonic larvae until the north limit of species distribution (Bartsch and Coombs, 1997; Gysels et al., 2004; Bonhommeau et al., 2008).

As a final remark, it is worth to note that complex life-history traits and patterns of migration impose a greater challenge to the study of connectivity patterns and gene flow. Aspects such as demographic disequilibrium, unbalanced sampling and low sample sizes of some populations can lead to a false interpretation of population homogeneity (type II error) (Waples, 1998). Thus, the interpretation of the data must be carried out with redoubled attention. To cover the complexity of *C. ramada'* life cycle, the next steps of this research should look to increase the spatial coverage, either in terms of sampling sites and sample size. Also, other molecular techniques such as high throughput sequencing may be used in future studies to attain a more complete overview. Moreover, in terms of the demographic dynamics it is important to understand the contribution of adults and larvae dispersal to the gene flow.

5. Conclusion

An increasing river fragmentation by in-stream barriers have been deteriorating riverine-marine connectivity and large part of the populations are now confined to the estuaries. The commercial exploitation in the Atlantic region has been low, but an intensification of their exploitation allied with species gregarious behaviour can lead to a dramatic reduction of population' sizes. This is of particular concern in the Portuguese coast since results attained in the present study show that those populations maintained a high gene flow with the remaining regions and seem to be central for the connectivity between Mediterranean Sea and Northeast Atlantic populations, like for other species such as the meagre *Argyrosomus regius* (Asso, 1801) (Almeida et al., 2022). So, fluctuations in this population's size may lead to restricted gene flow and isolation by distance, which may further hinder stock maintenance and species' ability to recover. Thus, it is essential to ensure that freshwater habitats are available, the riverine connectivity is not diminished, and that effective population sizes and fishing catches are monitored under marine and river basin management programs. Moreover, future studies on species migration and dispersion at sea are required to establish the link between population dynamics, spawning areas, gene flow and species' population conservation.

Funding

Funding was provided by the Portuguese Science Foundation (FCT) through the multiannual funding program contract of the UID MARE (Marine and Environmental Sciences Centre), via project UIDB/04292/2020, and under the project LA/P/0069/2020 granted to the Associate Laboratory ARNET. FCT also supported this study through a doctoral grant, cofunded by FSE through the "Programa Operacional Regional do Alentejo", attributed to E. Pereira (SFRH/BD/121042/2016); and individual contracts attributed to Catarina S. Mateus within the project "EVOLAMP - Genomic footprints of the evolution of alternative life histories in lampreys" (PTDC/BIA-EVL/30695/2017), and Bernardo R. Quintella (2020.02413.CEECIND).

CRediT authorship contribution statement

Esmeralda Pereira: Project administration, Investigation, Formal analysis, Data curation, Conceptualization, Visualization, Writing – original draft, Writing – review & editing. **Catarina S. Mateus:** Visualization, Validation, Supervision, Resources, Project administration, Methodology, Funding acquisition, Formal analysis, Conceptualization, Writing – review & editing. **Maria J. Alves:** Validation, Resources, Funding acquisition, Methodology, Writing – review & editing. **Rita Almeida:** Visualization, Validation, Formal analysis, Investigation, Writing – review & editing. **Joana Pereira:** Investigation, Writing – review & editing. **Bernardo R. Quintella:** Visualization, Validation, Supervision, Project administration, Conceptualization, Funding acquisition, Writing – review & editing. **Pedro R. Almeida:** Validation, Supervision, Resources, Project administration, Funding acquisition, Conceptualization, Writing – review & editing.

Declaration of competing interest

The authors declare that they have no known competing financial interests or personal relationships that could have appeared to influence the work reported in this paper.

Data availability

Data will be made available on request.

Acknowledgements

The authors wish to thank to Jean Durand for the valuable insights at the beginning of this study and to all researchers that provided samples, namely Daniel Golani (Hebrew University of Jerusalem), Emmanuil Koutrakis (Fisheries Research Institute, Hellenic Agricultural Organisation), Jan Breine (Research Institute for Nature and Forest), Laura Mura (AGRIS Sardegna), and William Roche (Inland Fisheries Ireland). As well as to the colleagues Andreia Domingues, Filipa Silva, José Pereira, Lurdes Pereira, Margarida Antunes, Amigos Pró-Lis and commercial fishermen that contributed to the sampling campaigns.

Appendix A. Supplementary data

Supplementary data to this article can be found online at https://doi.org/10.1016/j.ecss.2022.108209.

References

Almeida, P.R., Costa, M.I., Moreira, F., Assis, C.A., Costa, I.L., Gonçalves, I., 1992. *Liza Ramada (Risso, 1826) (Pisces: Mugilidae) No Estuário Do Tejo.* Um Recurso Subaproveitado. Publicações Avulsas do I.N.I.P.

Almeida, P.R., 1996. Estuarine movement patterns of adult thin-lipped grey mullet, *Liza ramada* (Risso) (Pisces: mugilidae), observed by ultrasonic tracking. J. Exp. Mar. Biol. Ecol. 202, 137–150. https://doi.org/10.1016/0022-0981(95)00162-X.

Almeida, P.R., 2003. Feeding ecology of Liza ramada (Risso, 1810) (Pisces, Mugilidae) in a south-western estuary of Portugal. Estuar. Coast Shelf Sci. 57, 313–323. https://doi.org/10.1016/S0272-7714(02)00357-8.

Almeida, R., Mateus, C.S., Alves, M.J., Marques, J.P., Pereira, J., Prista, N., Cabral, H., Almeida, P.R., Quintella, B.R., 2022. Evidence of genetic segregation among meagre (*Argyrosomus regius*) atlantic spawning areas. J. Mar. Sci. Eng. 10 (12), 1843. https://doi.org/10.3390/jmse10121843.

Als, T.D., Hansen, M.M., Maes, G.E., Castonguay, M., Riemann, L., Aarestrup, K., Munk, P., Sparholt, H., Hanel, R., Bernatchez, L., 2011. All roads lead to home: panmixia of European eel in the Sargasso Sea. Mol. Ecol. 20 (7), 1333–1346. https://doi.org/10.1111/j.1365-294X.2011.05011.x.

Ávila-Herrera, C.L., Pacheco-Almanzar, E., Guevara-Chumacero, L.M., Velázquez-Aragón, Serrato-Díaz, A., Ramírez-Saad, H., Ibánez, A.L., 2021. Past and recent connectivity of white mullet between the Gulf of Mexico and the Mexican Pacific inferred through sequences of the gene cytochrome c oxidase I and microsatellites. Mar. Biol. 168 (95), pp1–16. https://doi.org/10.1007/s00227-021-03907-x.

Bacheler, N.M., Wong, R.A., Buckel, J.A., 2005. Movements and mortality rates of striped mullet in North Carolina. N. Am. J. Fish. Manag. 25 (1), 361–373. https://doi.org/10.1577/M04-033.1.

Bartsch, J., Coombs, S., 1997. A numerical model of the dispersion of blue whiting larvae, Micromesistius potassiou (Risso) in the eastern North Atlantic. Fish. Oceanogr. 6, 141–154. https://doi.org/10.1046/j.1365-2419.1997.00036.x.

Bartulović, V., Glamuzina, B., Lucic, D., Conides, A., Jasprica, N., DulČiĆ, J., 2007. Recruitment and food composition of juvenile thin-lipped grey mullet, *Liza ramada* (Risso, 1826), in the Neretva River estuary (Eastern Adriatic, Croatia). Acta Adriat. 48 (1), 25–37.

Baselga, A., Gómez-Rodríguez, C., Araújo, M.B., Castro-Insua, A., Arenas, M., Posada, D., Vogler, A.P., 2022. Joint Analysis of Species and Genetic Variation to Quantify the Role of Dispersal and Environmental Constraints in Community Turnover. Ecography, e05808. https://doi.org/10.1111/ecog.05808.

Behrouz, M., Norouzi, M., Samiei, M.H., Pouria, H., 2018. Microsatellite analysis of golden grey mullet *Chelon auratus* (Risso, 1810) in the Fereydoon-Kenar and Ramsar coasts (south Caspian Sea, Iran). Croatian J. Fisheries. 76 (1), 35–40. https://doi.org/10.2478/cjf-2018-0004.

Belkhir, K., Borsa, P., Chikhi, L., Raufaste, N., Bonhomme, F., 2004. GENETIX 4.05, logiciel sous Windows TM pour la Génétique des Populations, Interactions, CNRS UMR 5000. Université de Montpellier II, Montpellier. Available at: http://www.genetix.univmontp2.fr/genetix/intro.htm.

Bonhommeau, S., Chassot, E., Rivot, E., 2008. Fluctuations in European eel (*Anguilla anguilla*) recruitment resulting from environmental changes in the Sargasso Sea. Fish. Oceanogr. 17 (1), 32–44. https://doi.org/10.1111/j.1365-2419.2007.00453.x.

Bower, A.S., Le Cann, B., Rossby, T., Zenk, W., Gould, J., Speer, K., Richardson, P.L., Prater, M.D., Zhang, H.M., 2002. Directly measured mid-depth circulation in the northeastern North Atlantic Ocean. Nature 419 (6907), 603–607. https://doi.org/10.1038/nature01078.

Brito, J.A., 2018. Population Genetic Structure and Connectivity Patterns of the Kanae (Mugil cephalus) in New Zealand Inland and Coastal Waters. Doctoral thesis, University of Wellington.

Bruslé, J., 1981. Food and feeding in grey mullets. In: Oren, O. (Ed.), Aquaculture of Grey Mullets. Cambridge University Press, Cambridge, pp. 185–217.

Cardona, L., 2016. Food and feeding of mugilidae. In: Crosett, D., Blaber, S.J. M. (Eds.), Biology, Ecology and Culture of Grey Mullet (Mugilidae). CRC Press, Boca Raton, USA. S.

Cardona, L., Hereu, B., Torras, X., 2008. Juvenile bottlenecks and salinity shape grey mullet assemblages in Mediterranean estuaries. Estuar. Coast Shelf Sci. 77 (4), 623–632. https://doi.org/10.1016/j.ecss.2007.10.018.

Chapman, D.D., Feldheim, K.A., Papastamatiou, Y.P., Hueter, R.E., 2015. There and back again: a review of residency and return migrations in sharks, with implications for population structure and management. Ann. Rev. Mar. Sci 7, 547–570. https://doi.org/10.1146/annurev-marine-010814-015730.

Chapuis, M.P., Estoup, A., 2007. Microsatellite null alleles and estimation of population differentiation. Mol. Biol. Evol. 24, 621–663. https://doi.org/10.1093/molbev/msl191.

Chauvet, C., Lasserre, G., Bach, P., Besseau, L., 1992. Résultats d'une expérience de marquage de trois especes de Poissons côtiers du Golf du Lion: Dicentrarchus labrax, Sparus aurata et Liza aurata. Cybium 16, 3–11.

Claridge, P.N., Potter, I.C., Hardisty, M.W., 1986. Seasonal changes in movements, abundance, size composition and diversity of the fish fauna of the Severn estuary. J. Mar. Biol. Assoc. U. K. 66 (1), 229–258. https://doi.org/10.1017/S002531540003976X.

Colín, A., Hernández-Pérez, Z., Guevara-Chumacero, L.M., Castañeda-Rico, S., Serrato-Díaz, A., Ibáñez, A.L., 2020. Are striped mullet (*Mugil cephalus*) philopatric? Mar. Biol. 167 (10) https://doi.org/10.1007/s00227-019-3622-1.

Cossu, P., Mura, L., Scarpa, F., Lai, T., Sanna, D., Azzena, I., Fois, N., Casu, M., 2021. Genetic patterns in *Mugil cephalus* and implications for fisheries and aquaculture management. Sci. Rep. 11, 2887. https://doi.org/10.1038/s41598-021-82515-7.

Cuéllar-Pinzón, J., Presa, P., Hawkins, S.J., Pita, A., 2016. Genetic markers in marine fisheries: types, tasks and trends. Fish. Res. 173 (3), 194–205. https://doi.org/10.1016/j.fishres.2015.10.019.

Daverat, F., Martin, J., Fablet, R., Pécheyran, C., 2011. Colonisation tactics of three temperate catadromous species, eel *Anguilla anguilla*, mullet *Liza ramada* and flounder *Platichthys flesus*, revealed by Bayesian multielemenal otolith microchemistry approach. Ecol. Freshw. Fish 20 (1), 42–51. https://doi.org/10.1111/j.1600-0633.2010.00454.x.

DeWoody, J.A., Avise, J.C., 2000. Microsatellite variation in marine, freshwater and anadromous fishes compared with other animals. J. Fish. Biol. 56 (3), 461–473. https://doi.org/10.1111/j.1095-8649.2000.tb00748.x.

Duong, T.Y., Uy, S., Chheng, P., So, N., Tran, T.H.T., Nguyen, N.T.T., Pomerroy, R., Egna, H., 2019. Genetic diversity and structure of striped snakehead (*Channa striata*) in the Lower Mekong Basin: implications for aquaculture and fisheries management. Fish. Res. 218, 166–173. https://doi.org/10.1016/j.fishres.2019.05.014.

Durand, J.-D., Blel, H., Shen, K.N., Koutrakis, E.T., Guinand, B., 2013. Population genetic structure of *Mugil cephalus* in the Mediterranean and Black Seas: a single mitochondrial clade and many nuclear barriers. Mar. Ecol. Prog. Ser. 474, 243–261. https://doi.org/10.3354/meps10080.

Earl, D.A., VonHoldt, B.M., 2012. Structure HARVESTER: a website and program for visualizing STRUCTURE output and implementing the Evanno method. Conserv. Genetics Resour. 4, 359–361. https://doi.org/10.1007/s12686-011-9548-7.

Evanno, G., Regnaut, S., Goudet, J., 2005. Detecting the number of clusters of individuals using the software STRUCTURE: a simulation study. Mol. Ecol. 14 (8), 2611–2620. https://doi.org/10.1111/j.1365-294X.2005.02553.x.

Excoffier, L., Lischer, H.E.L., 2010. Arlequin suite ver 3.5: a new series of programs to perform population genetics analyses under Linux and Windows. Mol. Ecol. Res. 10 (3), 564–567. https://doi.org/10.1111/j.1755-0998.2010.02847.x.

Feutry, P., Vergnes, A., Broderick, D., Lambourdiére, J., Keith, P., Ovenden, R., 2013. Stretched to the limit; can a short pelagic larval duration connect adult populations of an Indo-Pacific diadromous fish (*Kuhlia rupestris*)? Mol. Ecol. 22 (6), 1518–1530. https://doi.org/10.1111/mec.12192.

Frisk, M.G., Jordaan, A., Miller, T.J., 2014. Moving beyond the current paradigm in marine population connectivity: are adults the missing link? Fish Fish. 15 (2), 242–254. https://doi.org/10.1111/faf.12014.

Gallagher, B.K., Piccoli, P.M., Secor, D.H., 2018. Ecological carryover effects associated with partial migration in white perch (*Morone americana*) within the Hudson River Estuary. Estuar. Coast Shelf Sci. 200, 277–288. https://doi.org/10.1016/j.ecss.2017.11.011.

Guo, X.Z., Chen, H.M., Wang, A.B., Qian, X.Q., 2022. Population genetic structure of the yellow catfish (*Pelteobagrus fulvidraco*) in China inferred from microsatellite analyses: implications for fisheries management and breeding. J. World Aquacult. Soc. 53, 174–191. https://doi.org/10.1111/jwas.12844.

Gross, M.R., Coleman, R.M., McDowall, R.M., 1988. Aquatic productivity and the evolution of diadromous fish migration. Science 239, 1291–1293. https://doi.org/10.1126/science.239.4845.1291.

Gysels, E.S., Hellemans, B., Pampoulie, C., Volckaert, F.A., 2004. Phylogeography of the common goby, *Pomatoschistus microps*, with particular emphasis on the colonization of the Mediterranean and the North Sea. Mol. Ecol. 13 (2), 403–417. https://doi.org/10.1046/j.1365-294X.2003.02087.x.

Harrison, T.D., Cooper, J.A.G., 1991. Active migration of juvenile grey mullet (Teleostei: mugilidae) into a small lagoonal system on the Natal coast. South Afr. J. Sci. 87, 395–396.

Huey, J., Espinoza, T., Hughes, J.M., 2013. Regional panmixia in the mullet *mugil cephalus* along the coast of Eastern Queensland; revealed using six highly polymorphic microsatellite loci. Royal Soc. Queensland. Proceed. 118, pp7–15. Available: http://hdl.handle.net/10072/60521.

Hughes, J.M., Schmidt, D.J., Macdonald, J.I., Huey, J.A., Crook, D.A., 2014. Low interbasin connectivity in a facultatively diadromous fish: evidence from genetics and otolith chemistry. Mol. Ecol. 23 (5), 1000–1013. https://doi.org/10.1111/mec.12661.

Islam, M.R., Schmidt, D.J., Crook, D.A., Hughes, J.M., 2018. Patterns of genetic structuring at the northern limits of the Australian smelt (*Retropinna semoni*) cryptic species complex. PeerJ. https://doi.org/10.7717/peerj.4654.

Jamandre, B.W., Durand, J.M., Tzeng, W.N., 2009. Phylogeography of the flathead mullet *Mugil cephalus* in the north-west Pacific as inferred from the mtDNA control region. J. Fish. Biol. 75 (2), 393–407. https://doi.org/10.1111/j.1095-8649.2009.02332.x.

Jakobsen, P.K., Ribergaard, M.H., Quadfasel, D., Schmith, T., Hughes, C.W., 2003. Near-surface circulation in the northern North Atlantic as inferred from Lagrangian drifters: variability from the mesoscale to interannual. J. Geophys. Res. 108 (C8), 3251. https://doi.org/10.1029/2002JC001554.

Jerry, D.R., Baverstock, P.R., 1998. Consequences of a catadromous life-strategy for levels of mitochondrial DNA differentiation among populations of the Australian bass, *Macquaria novemaculeata*. Mol. Ecol. 7 (8), 1003–1013. https://doi.org/10.1046/j.1365-294x.1998.00418.x.

Jonsson, B., Jonsson, N., 2008. Thinlip grey mullet *Liza ramada* (Mugilidae) caught in a small Norwegian stream. Fauna Nor. 26/27 (1), 31–33. https://doi.org/10.5324/fn.v26i0.571.

Kaimuddin, A.H., Laë, R., De Morais, L.T., 2016. Fish species in a changing world: the route and timing of species migration between tropical and temperate ecosystems in eastern atlantic. Front. Mar. Sci. 3 (162) https://doi.org/10.3389/fmars.2016.00162.

Kasapidis, P., Silva, A., Zampicinini, G., Magoulas, A., 2012. Evidence for microsatellite hitchhiking selection in European sardine (Sardina pilchardus) and implications in inferring stock structure. Sci. Mar. 76, 123–132. https://doi.org/10.3989/scimar.03366.29B.

Keenan, K., McGinnity, P., Cross, T.F., Crozier, W.W., Prodöhl, P.A., 2013. diveRsity: an R package for the estimation and exploration of population genetics parameters and their associated errors. Methods Ecol. Evol. 4 (8), 782–788. https://doi.org/10.1111/2041-210X.12067.

Kingsford, M.J., Suthers, I.M., 1994. Dynamic estuarine plumes and fronts: importance to small fish and plankton in coastal waters of NSW, Australia. Continent. Shelf Res. 14, 655–672. https://doi.org/10.1016/0278-4343(94)90111-2.

Koutrakis, E., 2016. Biology and ecology of fry and juveniles of mugilidae. In: Crosetti, D., Blaber, S. (Eds.), Biology, Ecology and Culture of Mullets (Mugilidae). CRC Press, Boca Raton, USA, pp. 27–263.

Leclerc, E., Mailhot, Y., Mingelbier, M., Bernatchez, L., 2008. The landscape genetics of yellow perch (Perca flavescens) in a large fluvial ecosystem. Mol. Ecol. 17 (7), 1702–1717. https://doi.org/10.1111/j.1365-294X.2008.03710.x.

Lemonnier, A., 2019. Volet poissons migrateurs 2015-2021: Dynamique de la population de Mulet porc (Chelon ramada) dans le bassin versant de la Vilaine – 2019. Etablissement Public Territorial du Bassin de la Vilaine (EPTB), p. 39p.

Limborg, M.T., Hanel, R., Debes, P.V., Ring, A.K., André, C., Tsigenopoulos, C.S., Bekkevold, D., 2012. Imprints from genetic drift and mutation imply relative divergence times across marine transition zones in a pan-European small pelagic fish (Sprattus sprattus). Heredity 109 (2), 96–107. https://doi.org/10.1038/hdy.2012.18.

Liu, L., Gao, T.X., Han, Z.Q., Li, C.H., Sun, D.R., Song, N., 2016. Development and characterization of microsatellite markers of the eastern keelback mullet (*Liza affinis*). Genet. Mol. Res. 15 (2), 1–4. https://doi.org/10.4238/gmr.15028380.

Liu, L., Zhang, X., Sun, D., Gao, T., Song, N., 2019. Population genetic structure of *Liza affinis* (Eastern Keelback Mullet), reveals high gene flow inferred from microsatellite analysis. Ocean Sci. J. 54, 245–256. https://doi.org/10.1007/s12601-019-0013-y.

Lui, J.-Y., Lun, Z.-R., Zhang, J.-B., Yang, T.-B., 2009. Population genetic structure of striped mullet, *Mugil cephalus*, along the coast of China, inferred by AFLP fingerprinting. Biochem. Systemat. Ecol. 37 (4), 266–274. https://doi.org/10.1016/j.bse.2009.04.010.

Mai, A.C., Mino, C.I., Marins, L.F., Monteiro-Neto, C., Miranda, L., Schwingel, P.R., Lemos, V.M., Gonzalvez-Castro, M., Castello, J.P., Vieira, J.P., 2014. Microsatellite variation and genetic structuring in *Mugil liza* (Teleostei: mugilidae) populations from Argentina and Brazil. Estuar. Coast Shelf Sci. 149, 80–86. https://doi.org/10.1016/j.ecss.2014.07.013.

Maes, G.E., Volckaert, F.A.M., 2007. Challenges for genetic research in European eel management. ICES (Int. Counc. Explor. Sea) J. Mar. Sci. 64 (7), 1463–1471. https://doi.org/10.1093/icesjms/fsm108.

McDowall, R.M., 1997. The evolution of diadromy (revisited) and its place in phylogenetic analysis. Rev. Fish Biol. Fish. 7, 443–462. https://doi.org/10.1023/A:1018404331601.

Menna, M., Poulain, P.-M., Ciani, D., Doglioli, A., Notarstefano, G., Gerin, R., Rio, M.-H., Santoleri, R., Gauci, A., Drago, A., 2019. New insights of the Sicily Channel and southern tyrrhenian sea variability. Water 11 (7), 1355. https://doi.org/10.3390/w11071355.

Mires, D., Shak, Y., Shilo, S., 1974. Further observations on the effect of salinity and temperature changes on *Mugil capito* and *Mugil cephalus* fry. Bamidgeh 26, 104–109.

Naderi, L., Shabani, A., Imsiridou, A., 2017. Genetic diversity of sharpnose *mullet Liza saliens* introduced in southern Caspian Sea in comparison with one native Aegean Sea population. J. Ichthyol. 57, 297–305. https://doi.org/10.1134/S0032945217020126.

Neethling, M., Matthee, C.A., Bowie, R.C., von der Heyden, S., 2008. Evidence for panmixia despite barriers to gene flow in the southern African endemic, *Caffrogobius caffer* (Teleostei: gobiidae). BMC Evol. Biol. 8, 325. https://doi.org/10.1186/1471-2148-8-325.

Nelson, J.S., 2006. Fishes of the World, fourth ed. John Wiley and Sons, Inc., New Jersey.

O'Dwyer, J.E., Murphy, N., Tonkin, Z., Lyon, J., Koster, W., Dawson, D., Amtstaetter, F., Harrison, K.A., 2021. An investigation of genetic connectivity shines a light on the relative roles of isolation by distance and oceanic currents in three diadromous fish species. Mar. Freshw. Res. 72 (10), 1457–1473. https://doi.org/10.1071/MF20323.

Oliveira, J.M., Ferreira, M.T., 1997. Abundance, size composition and growth of a thinlipped grey mullet, *Liza ramada* (Pisces: mugilidae) population in an Iberian River. Folia Zoologica 46 (4), 375–384.

Ordeix, M., Pou-Rovira, Q., Sellarès, N., Bardina, M., Casamitjana, A., Solà, C., Munné, A., 2011. Fish pass assessment in the rivers of Catalonia (NE Iberian Peninsula). 'A case study of weirs associated with hydropower plants and gauging stations. Limnética 30 (2), 405–426. https://doi.org/10.23818/limn.30.29.

Oren, O.H., 1981. Aquaculture of Grey Mullets. International Biological Programme26. Cambridge University Press, Cambridge, Great Britain, p. 507pp.

Pacheco-Almanzar, E., Ramírez-Saad, H., Velázquez-Aragón, J.A., Serrato, A., Ibáñez, A. L., 2017. Diversity and genetic structure of white mullet populations in the Gulf of Mexico analyzed by microsatellite markers. Estuar. Coast Shelf Sci. 198, 249–256. https://doi.org/10.1016/j.ecss.2017.09.015.

Palero, F., Abelló, P., Macpherson, E., Gristina, M., Pascual, M., 2008. Phylogeography of the European spiny lobster (Palinurus elephas): influence of current oceanographical features and historical processes. Mol. Phylogenet. Evol. 48 (2), 708–717. https://doi.org/10.1016/j.ympev.2008.04.022.

Peakall, R., Smouse, P.E., 2012. GenAlEx 6.5: genetic analysis in Excel. Population genetic software for teaching and research–an update. Bioinformatics 28 (19), 2537–2539. https://doi.org/10.1093/bioinformatics/bts460.

Pereira, E., Quintella, B.R., Lança, M.J., Alexandre, C.M., Mateus, C.S., Pedro, S., Belo, A. F., Rato, A.S., Quadrado, M.F., Telhado, A., Batista, C., Almeida, P.R., 2021. Temporal patterns of the catadromous thinlip grey mullet migration in freshwater. Ecohydrology 14 (8), e2345. https://doi.org/10.1002/eco.2345.

Pritchard, J.K., Stephens, M., Donnelly, P., 2000. Inference of population structure using multilocus genotype data. Genetics 155 (2), 945–959. https://doi.org/10.1093/genetics/155.2.945.

Piry, S., Luikart, G., Cornuet, J.M., 1999. BOTTLENECK: a computer program for detecting recent reductions in the effective population size using allele frequency data. J. Hered. 90 (4), 502–503. https://doi.org/10.1093/jhered/90.4.502.

Prandle, D., Ballard, G., Flatt, D., Harrison, A.J., Jones, S.E., Knight, P.J., Loch, S., McManus, J., Player, R., Tappin, A., 1996. Combining modelling and monitoring to determine fluxes of water, dissolved and particulate metals through the Dover Strait. Continent. Shelf Res. 16 (2), 237–257. https://doi.org/10.1016/0278-4343(95)00009-.

Rosenberg, N.A., 2004. Distruct: a program for the graphical display 475 of population structure. Mol. Ecol. Notes 4 (1), 137–138. https://doi.org/10.1046/j.1471-8286.2003.00566.x.

Sá-Pinto, A., Branco, M.S., Alexandrino, P.B., Fontaine, M.C., Baird, S.J.E., 2012. Barriers to gene flow in the marine environment: insights from two common intertidal limpet species of the Atlantic and Mediterranean. PLoS One 7 (12), e50330. https://doi.org/10.1371/journal.pone.0050330.

Sauriau, P.-G., Robin, J.-P., Marchand, J., 1994. Effects of the excessive organic enrichment of the Loire Estuary on the downstream migratory patterns of the amphihaline grey mullet (*Liza ramada*) (Pisces: mugilidae). In: Dyer, K.R., Orth, R.J. (Eds.), *Changes In Fluxes In Estuaries (ECSA22/ERF Symposium)*, Olsen and Olsen, pp. 349–356. Fredensborg, Denmark.

Shen, K.N., Chen, C.Y., Tzeng, W.N., Chen, J.D., Knibb, W., Durand, J., 2010. Development and characterization of 13 GT/CA microsatellite loci in cosmopolitan flathead mullet Mugil cephalus', in: permanent genetic resources added to molecular ecology resources database 1April2010-31May 2010. Mol. Ecol. Res. 10 (6), 1098–1105. https://doi.org/10.1111/j.1755-0998.2010.02898.x.

Shen, K.N., Jamandre, B.W., Hsu, C.C., Tzeng, W.-N., Durand, J.-D., 2011. Plio-Pleistocene sea level and temperature fluctuations in the northwestern Pacific promoted speciation in the globally-distributed flathead mullet *Mugil cephalus*. BMC Evol. Biol. 11 (83) https://doi.org/10.1186/1471-2148-11-83.

Thomson, J.M., 1966. The grey mullets. Oceanogr. Mar. Biol. Annu. Rev. 4, 301–355.

Tintoré, J., La Violette, P.E., Blade, I., Cruzado, A., 1988. A study of an intense density front in the eastern Alboran Sea: the Almeria–Oran front. J. Phys. Oceanogr. 18 (10), 1384–1397. https://doi.org/10.1175/1520-0485(1988)018<1384:ASOAID>2.0.CO;2.

Van Oosterhout, C., Hutchinson, W.F., Wills, D.P., Shipley, P., 2004. MICRO-CHECKER: software for identifying and correcting genotyping errors in microsatellite data. Mol. Ecol. Notes 4 (3), 535–538. https://doi.org/10.1111/j.1471-8286.2004.00684.x.

Wallace, J.H., 1975. The estuarine fishes of the east coast of South Africa. I. Species composition and length distribution in the estuarine and marine environments. II. Seasonal abundance and migrations. Investig. Rep. Oceanographic Res. Inst. 40, 1–72.

Waples, R.S., 1998. Separating the wheat from the chaff: patterns of genetic differentiation in high gene flow species. J. Hered. 89, 438–450. https://doi.org/10.1093/jhered/89.5.438.

Werner, E.E., Gilliam, J.F., 1984. The ontogenetic niche and species interactions in size structured populations. Annu. Rev. Ecol. Systemat. 15, 393–425.

Whitfield, A.K., Panfili, J., Durand, J.D., 2012. A global review of the cosmopolitan flathead mullet *Mugil cephalus* Linnaeus 1758 (Teleostei: mugilidae), with emphasis on the biology, genetics, ecology and fisheries aspects of this apparent species complex. Rev. Fish Biol. Fish. 22 (3), 641–681. https://doi.org/10.1007/s11160-012-9263-9.

Xu, G., Shao, C., Liao, X., Tian, Y., Chen, S., 2009. Isolation and charaterization of polymorphic microsatellite loci from soiuy mullet (*Mugil soiuy* Basilewsky 1855). Conserv. Genet. 10 (3), 653–655. https://doi.org/10.1007/s10592-008-9602-5.

Xu, T.J., Sun, D.Q., Shi, G., Wang, R.X., 2010. Development and characterization of polymorphic microsatellite markers in the grey mullet (Mugil cephalus). Genet. Mol. Res. 9 (3), 1791–1795. https://doi.org/10.3732/ajb.1000153.

Yoshimatsu, T., Matsui, S., Kitajima, C., 1993. Early development of laboratory–reared keelback mullet. Nippon Suisan Gakk 59 (5), 765–776.